Simultaneous Control of Active and Reactive Powers of Vanadium Redox Flow Battery Systems in Flexible Microgrids

Majid Hosseina, Seyed Mohammad Taghi Bathaee, and Alireza Fereidunian

Abstract
This paper discusses the control of flexible microgrids, consisting of a Redox Flow Batteries (RFB) and a new power conditioning system (PCS) for the RFB. Considering the importance of energy storage, this study is essential in power systems that are developed cautiously. RFB is connected to power system by a DC/DC or DC/AC converter to produce a DC voltage. It is very important that this converter be effectively modeled and controlled for applications in microgrids. This paper focuses on simultaneous active and reactive power control in RFB systems. In this regard, this study proposes a new Flexible AC Transmission System (FACTS) compensator for microgrids which is able to control the active and reactive power. This type of compensator presents a good transient response. The simulation results, performed by Matlab-Simulink toolbox, show the validity of the proposed system.

Keywords**—**Redox flow battery (RFB), power conditioning system (PCS), flexible ac transmission system (FACTS), Microgrid.

I. INTRODUCTION

Microgrids include distributed generation (DG) sources, electrical energy storage systems (EES) and controllable loads. Microgrids are able to work when they are connected to the grid or in islanding mode. Distributed generation technology is flexible, clean, and environmentally friendly [1-2].

Storage devices play an important role in the operation of the microgrids. Each storage technology has some advantages, disadvantages and limitations. One of the limitations is range of application. RFB is one of the advanced batteries. Though, the development of Vanadium Redox Battery (VRB) is expanding the possibilities for large-scale storage facilities, which is suitable for modern power systems. RFB has the advantageous of flexibility in capacity and power. It is suitable for load leveling and uninterruptible power supply. RFB have a rapid response and would not age by charging and discharging [3-6].

Manuscript received May 13, 2014; revised October 1, 2014; accepted October 21, 2014.

M. Hosseina, Department of Electrical Engineering K. N. Toosi University of Technology, Tehran, Iran (email: majidhosseina@gmail.com)

Power Electronic Interface of a RFB in microgrids consists of DC-DC or DC-AC Converter. These converters control and regulate the DC or AC link of converters. They also control the flow direction of the power. In the storing operation mode RFB is charged and in the discharging mode power from the battery is injected into the network. In fact, to operate in both modes, the converters should be bidirectional. Therefore it is essential to effectively model and control these converters for the applications in microgrids [7].

The power conditioning system (PCS) is an interface that connects the VRB to the electric power system effectively [8-9]. The PCS provides a power electronic interface between the ac power system and the VRB. To achieve the following objectives, electric power should be converted either from DC to AC or from AC to DC. It is also needed to efficiently charge and discharge the VRB device.

Fig. 1.a shows the PCS configuration based on a 12-pulse bidirectional thyristor converter. In this system, the active power is controlled between VRB and network with current measurement. In fact, the thyristor converter operates as a current source on the dc side. Thus, this system does not require DC/DC converter. But it has some disadvantages such as slow response and inability to control the reactive power. Fig. 1.b shows a typical PCS configuration [7] which consists VSC, VRB and the interface between the VSC and the VRB, represented by a bidirectional DC/DC converter. VSC usually consists of six insulated gate bipolar transistors (IGBTs) with anti-parallel diodes. In previous studies, control of active power in the batteries was discussed. Also VRB just are known as active power source. In this regard, this paper proposes a new FACTS compensator based on bidirectional IGBT converter for controlling the exchange of active and reactive power flow between the VRB and the grid. This paper is structured as follows: the VRB model is developed in Section 2. The models of the proposed compensator and the corresponding control system are developed in Section 3. Then simulation results are performed in Section 4. Finally, the conclusions are presented in Section 5.

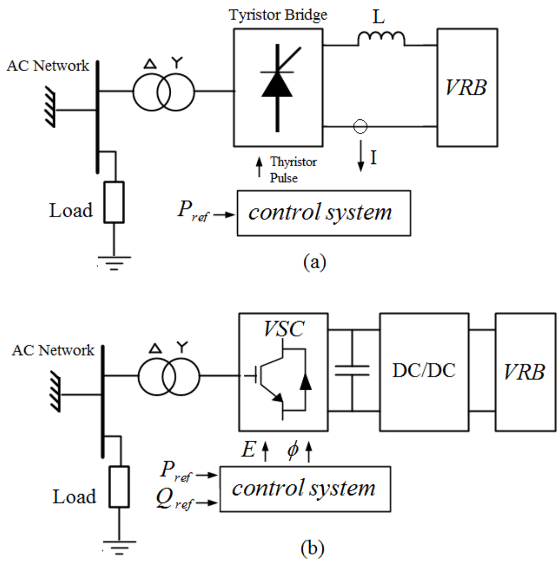

Fig. 1. Schematic of power conditioning system
a. Typical configuration
b. Proposed configuration

II. Redox Flow Batteries

A. RFB

Redox stands for reduction and oxidation combination. A flow battery is electrochemical equipment in which chemical energy is converted into electrical energy, similar to conventional batteries. The Electro-active materials in a flow battery are stored an electrolyte outside of it. VRFB has the electrolyte including these active materials in external containers, such as tanks, and charges and discharges electricity by supplying the electrolyte to the flow type cell by pumps or other means.

A schematic of a Redox flow battery system is shown in Fig. 2. Most Redox flow batteries consist of two separate electrolytes and a storing electro-active materials for separate the negative electrode reactions and the positive electrode reactions.

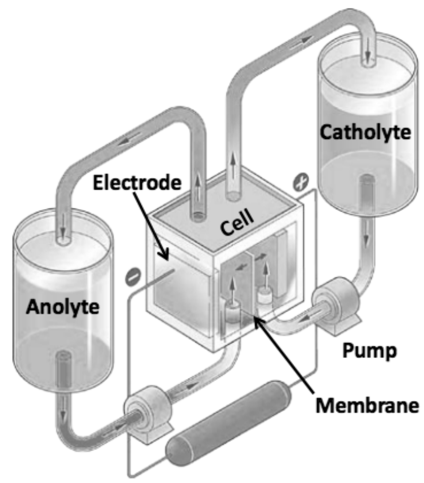

Fig. 2. Schematic of a redox flow battery system [10]

Metal ions that change capacity can be used in a redox system; however, with considering various factors such as economy, energy density and efficiency, the Vanadium batteries (V^{2+}/V^{3+}), the Iron batteries (Fe^{2+}/Fe^{3+}) and Chromium batteries (Cr^{3+}/Cr^{2+}) are favorable systems. The vanadium system is particularly advantageous because it uses the same metal ions at both positive and negative electrodes. Unlike a system with two different metal ions, such as iron and chromium, vanadium battery capacity does not decrease even when the electrolytes are mixed each other through the membrane. The vanadium system is thus currently widely developed around the world. For comparison RFB with other batteries the characteristics of the main battery storage technologies are shown in Table 1. Table.2 tabulates capacity of some installed RFB.

B. Vanadium Redox Flow Battery

In vanadium Redox flow battery (VRB), standard positive electrode potential is approximately +1.00V. The characteristic reaction of the all vanadium battery at the positive electrode, which includes soluble $V(IV)$ and $V(V)$ species, is as follows: (ions V^{4+} and V^{5+} are in fact vanadium oxide ions respectively VO^{2+} and VO_2^{+}) [11-18]:

$$VO^{2+} + H_2O - e^- \xleftrightarrow{charge\&discharge} VO_2^+ + 2H^+ \quad (1)$$

The reversible reaction at the negative electrode involves $V(II)$ and $V(III)$ species and has a standard potential of $-0.26V$:

$$V^{3+} + e^- \xleftrightarrow{charge\&discharge} V^{2+} \quad (2)$$

The general scheme of the VRB is shown in Fig. 3. By pumping the electrolyte in the battery circulated and chemical reactions occur. Table.3 shows some of the renowned flow battery systems.

The model used to represent dynamics of the VRB has been presented in more details in [15] and [16]. Fig.4. shows a simple model for the VRB that composed of two parts: the stack model (electrochemical model), and the mechanical model. In the stack model, the terminal current (I_{batt}) determines the stack current (I_{stack}), the terminal stack

TABLE I
Main battery storage technologies [11]

STORAGE TECHNOLOGY	LIFE TIME	EFFICIENCY	TIME SCALE
Flow battery	10000 cycles	75-80%	Minutes-Hours
Lithium-Ion	3000 cycles	97%	Seconds-Minutes
Sodium-Sulfur (NaS)	2200 cycles	89%	Minutes-Hours

TABLE II
Some installation records [12]

Capacity	Application
450kW/2h	Load-Leveling
100kW/8h	Load-Leveling
200kW/8h	Load-Leveling
170kW/6h	For Wind Turbine
3MW/1.5s	Voltage Sag Protection
1.5MW/1h	Load-Leveling
30kW/8h	Photo Voltaic
1.5MW/8h	Load-Leveling

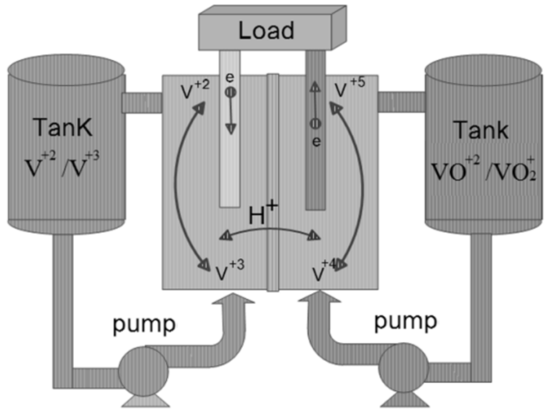

Fig. 3. Principle of a vanadium redox flow battery system

TABLE III
renowned flow battery

System	Reaction	E^0_{cell}
All Vanadium	$V^{2+} \leftrightarrow V^{3+} + e^-$ $VO^{2+} + e^- \leftrightarrow VO_2^{+}$	1.4 V
Vanadium-Polyamide	$V^{2+} \leftrightarrow V^{3+} + e^-$ $\frac{1}{2}Br_2 + e^- \leftrightarrow Br^-$	1.3 V
Iron-Chromium	$Fe^{2+} \leftrightarrow Fe^{3+} + e^-$ $Cr^{3+} + e^- \leftrightarrow Cr^{2+}$	1.2 V
Zinc-Bromine	$Zn \leftrightarrow Zn^{2+} + 2e^-$ $Br_2 + 2e^- \leftrightarrow 2Br^-$	1.8 V
Zinc-Cerium	$Zn \leftrightarrow Zn^{2+} + 2e^-$ $2Ce^{4+} + 2e^- \leftrightarrow 2Ce^{3+}$	2.4 V

voltage (V_{stack}) and the state of charge (*SOC*) of the electrolyte. In the mechanical model, by the external control system, the flow rate that produces a pressure drop in the hydraulic system is determined. Pumps that provide energy for electrolytic movement are two DC machines. Hence, current pumps (I_{Pumpe}), as the current consumption should be subtract from the current terminal. This model considers internal resistance and parasitic resistance. Internal resistance accounts for battery's losses such as membrane resistance, solution resistance, electrode resistance and etc. Parasitic resistance accounts for power consumption by recirculation pumps, the system controller, and power loss from cell stack by-pass currents.

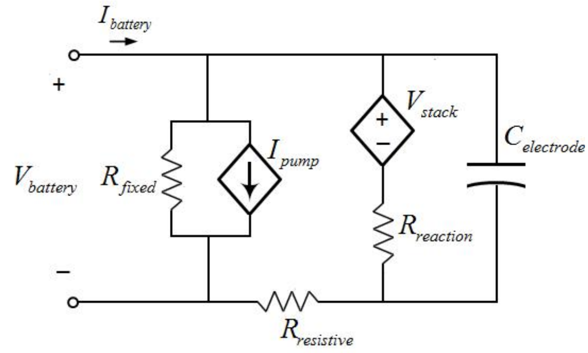

Fig. 4. Studied vanadium redox flow battery system model

Internal battery voltage is obtained from the following equation:

$$V_{battery} = n_{cell}(V_{eq} + \frac{2RT}{F}\ln(\frac{SOC}{1-SOC})) \quad (3)$$

where:

T - The temperature impact on battery operation;

R - The VRB internal resistance (in VRB cases the internal resistance is constant).

F - The Faraday's constant.

V_{eq} - Internal cell voltage when the (*SOC*) is 0.5 pu.

The state of charge is defined as:

$$SOC = \frac{E_c}{E_{total}} = SOC_0 + \int \frac{-V_{battery}I_{battery}}{E_{total}}dt \quad (4)$$

where:

E_c - Current energy in battery;

E_{total} - The total energy capacity.

The parasitic losses are divided into two parts: fixed losses (shown with a fixed resistance) and variable losses (shown with as a controlled current source that is dependent on the *SOC*. The losses are as follows:

$$P_{parasitic} = P_{fixed} + k(\frac{I_{stack}}{SOC}) \quad (5)$$

k is a coefficient that obtained from experimental results. The parasitic and pump losses are derived as follows:

$$R_{fixed} = \frac{V_{stack}^2}{P_{fixed}} \quad (6)$$

$$I_{pump} = \frac{k(\frac{I_{stack}}{SOC})}{V_{stack}} \quad (7)$$

III. ACTIVE AND REACTIVE POWER CONTROL

This study suggests $P-Q$ control system for the proposed PCS unit. The overall model of converter including VRB is shown in Fig. 5 [19-27].

Its mathematical model under dq coordinate system is:

$$u_d = s_d u_{dc} + \omega L i_q - R i_q - L\frac{di_d}{dt} \tag{8}$$

$$u_q = s_q u_{dc} - \omega L i_d - R i_d - L\frac{di_q}{dt} \tag{9}$$

where:

ω -angular frequency

u_d -direct axis voltage

u_q -quadrature axis voltage

s_d , s_q -duty cycle

i_d , i_q -direct axis and quadrature axis current

R -resistance

L -inductance

Equation (10) and (11) can be got after forward decoupled control.

$$u_{1d}^{'} = (k_{idp} + \frac{k_{idi}}{s})(i_d^* - i_d) - \omega L i_q + u_s \tag{10}$$

$$u_{1q}^{'} = (k_{idp} + \frac{k_{iqi}}{s})(i_d^* - i_d) - \omega L i_d \tag{11}$$

$u_{1d}^{'}$, $u_{1q}^{'}$ can be used as the driven signal for PWM inverter. u_s is the magnitude of voltage. Neglect the power loss of inverter's and forces u_q to be zero. With this assumption, equations (12) and (13) are obtained.

$$P = u_d i_d + u_q i_q = u_d i_d \tag{12}$$

$$Q = u_q i_d - u_d i_q = -u_d i_q \tag{13}$$

Because $u_d = u_s$, active power is proportional to i_d and Equation (14) can be got

$$i_d^* = (k_{pp} + \frac{k_{pi}}{s})(P^* - P) \tag{14}$$

$$i_q^* = -(k_{up} + \frac{k_{ui}}{s})(u^* - u) \tag{15}$$

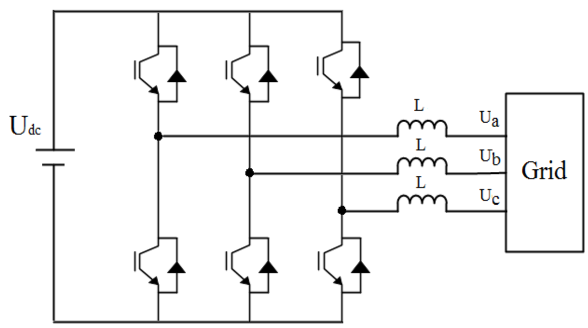

Fig.5. overall model of converter includes VRB

The output power can be represented by (16) and (17)

$$P_{ref} = u_d i_d \tag{16}$$

$$Q_{ref} = -u_d i_q \tag{17}$$

The reference value of DQ axis can be got:

$$i_{dref} = \frac{P_{ref}}{u_d} \tag{18}$$

$$i_{qref} = -\frac{Q_{ref}}{u_d} \tag{19}$$

Schematic of active power-voltage control and control structure are shown by Fig.6 and Fig.7 respectively.

IV. SIMULATION RESULT

The study system is depicted in Fig. 8. This model system is composed of a 132 kV bulk power system (represented as an infinite ac bus) connected to a 63 kV network by two power transformer. The 63 kV sub-system is comprised of a 4.4 MW constant load and a 1.8 MW (4×450 kW) PCS/VRB unit. Details of each part 450 kW are shown in Table.4.

Simulations have been performed for the following two cases.

A. Active power control

In this case PCS/VRB unit is like a current source that only controls active power. Due to constant load

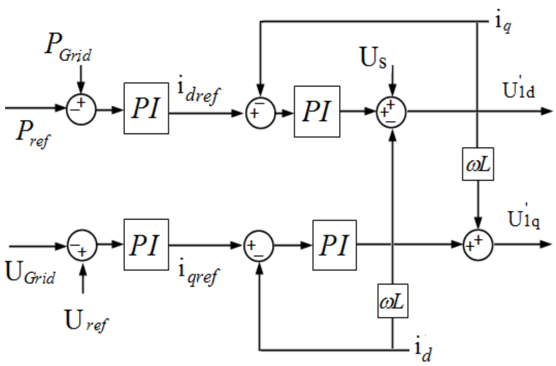

Fig.6. schematic of active and reactive power control

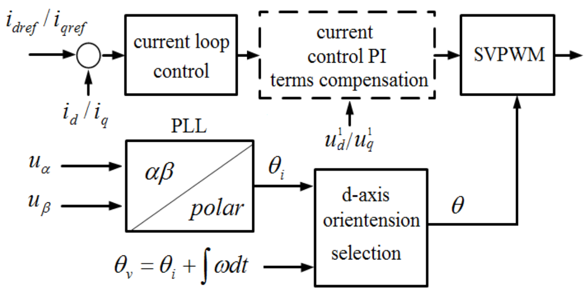

Fig.7. schematic of control Structure

power, total network's power and PCS/VRB unit consumption or production and losses, are equal to load consumption. Fig.9 and Fig.10 show active power and reactive power generated by the PCS/VRB unit and network, respectively. In this section, reactive power generated by the PCS/VRB unit is considered to be zero.

Simulation was performed for 6 seconds. During this period, active power load is 4.2 MW and reactive power load is 1.4 MVAR. In the first two seconds, the battery is discharged by nominal current. This period represents the time that the battery is charged and the full power injected into the grid. At this point, PCS/VRB unit and network produced 1.55 MW and 2.8 MW active powers, respectively. In the next two seconds, the battery is discharged nearly by 40% of the nominal current. When this happens, VRB generation active power is reduced to 0.65 MW and network generation active power is increased to 3.8 MW. Finally in the last two second, the battery is charged by nominal current. In this period, power network must generate 6.1 MW. According to this experiment, reactive power generated by the VRB is zero and all reactive power is provided by the grid. The VRB current and network current are shown in Fig. 10 and Fig. 11, respectively.

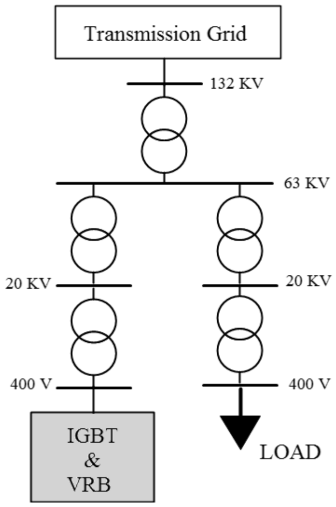

Fig. 8. Model power system

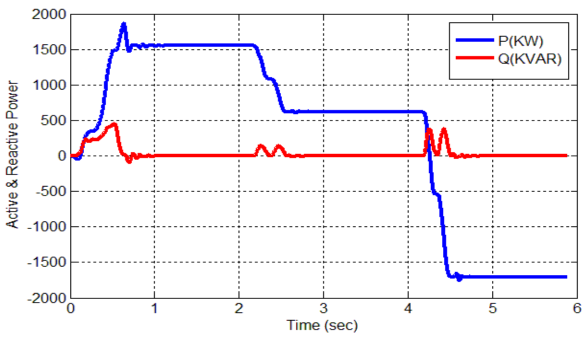

Fig. 9. Active power and reactive power generated by VRB

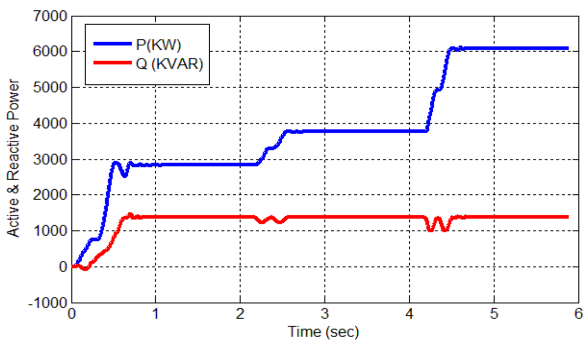

Fig. 10. Active power and reactive power generated by network

Notice that the two-second time periods, representatives of various modes of operation for PCS/VRB unit. Usually the VRB is not fully discharged and nominal discharge time, typically several hours. Hence, the battery can generate power to the grid during peak hours and charged to store energy in low load hours. This can be because of load leveling profile.

Fig. 12 shows the i_d and i_q of the proposed model. i_d i_d control active power and i_q control reactive power in PCS/VRB unit. Fig. 13 shows output phase voltage and Fig. 14 shows the inverter output line voltage. SVPWM method is used for switching.

B. Active and reactive power control

In this section active and reactive powers can be controlled simultaneously. In previous studies related

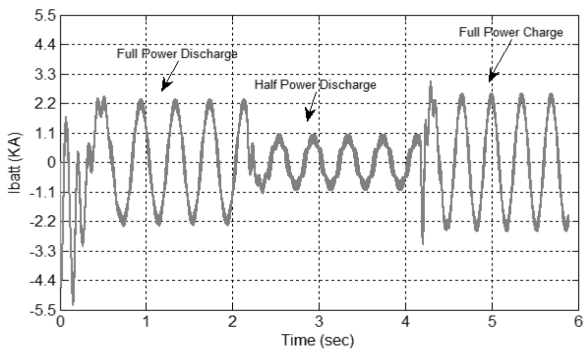

Fig. 11. VRB output current

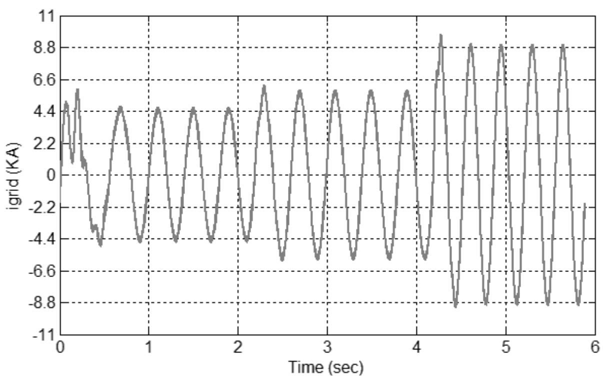

Fig. 11. AC network current

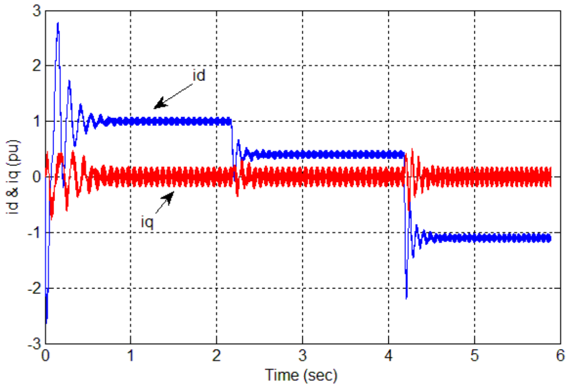

Fig. 12. i_d and i_q current in proposed model

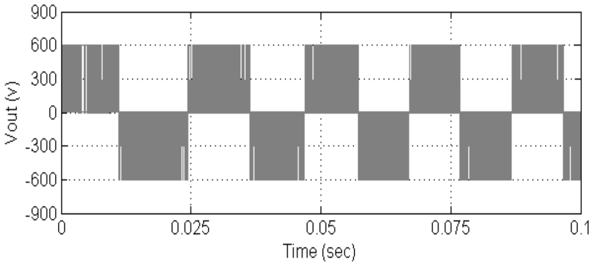

Fig. 13. Inverter output line voltage

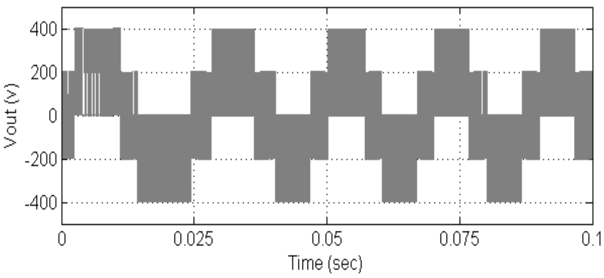

Fig. 14. Inverter output phase voltage

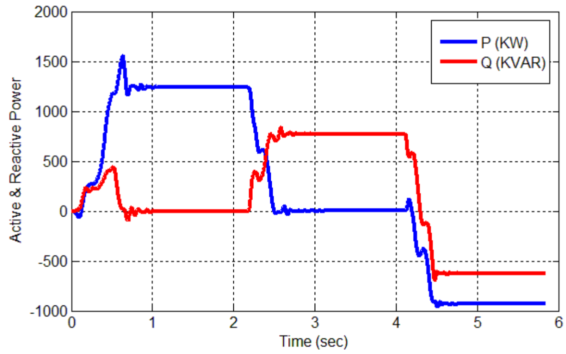

Fig. 15. Active power and reactive power generated by VRB

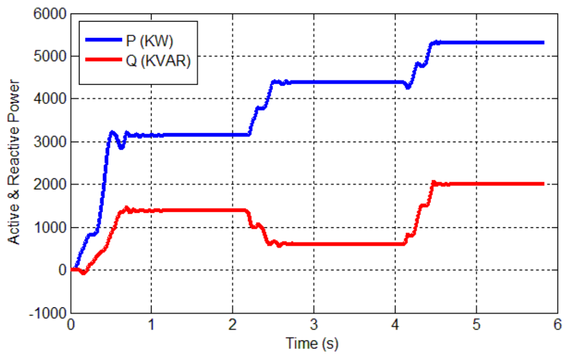

Fig. 16. Active power and reactive power generated by network

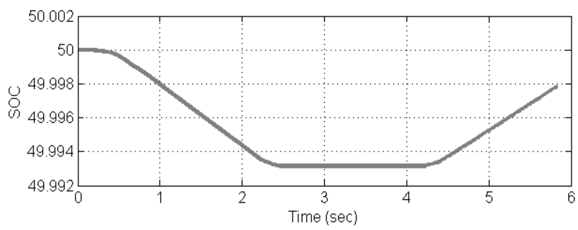

Fig. 17. State of charge (SOC) of the VRB

to the VRB, active power control was discussed. Note that VRB are continuously being charged and discharged and there are intervals that the VRB is charging and the network does not need to use it. At this time, VRB must be removed from the network but can be used VRB as a STATCOM and controlled the reactive power. The control method presented in this paper indicate that this mode. Fig.15 and Fig.16 show active power and reactive power generated by the PCS/VRB unit and network in this mode, respectively.

This section differs from the previous one in the second period (From 2s to 4s). This period represents the time that the VRB neither consume nor produce active power. However, as shown in Fig. 15, in this period PCS/VRB unit injects reactive power into the network and acts as a synchronous condenser. Fig.17 shows the state of charge (SOC) of the VRB. Initial charge of the battery is assumed to be 50%in the simulation. Fig. 17 shows the i_d and i_q of the proposed model for simultaneous control of active and reactive power.

According to Fig. 12 and Fig. 18, it is seen that the dynamic system response is rapid. The fast dynamic response and stability are the benefits of the system which is modeled in this paper. Fig.19 shows the voltage of the PCS/VRB unit bus. As is obvious, the reactive power generated by the PCS/VRB unit increases the voltage. Fig.20 shows the voltage of 63kV bus. As is known in the second period PCS/VRB unit improves the voltage profile.

V. Conclusion

This paper proposes a new PCS unit for the VRB. The PCS controls the active and reactive powers. This paper was focused on control the active power and reactive power simultaneously in PCS/VRB unit. In fact, the proposed PCS/VRB unit plays the role of DG and STATCOM at the same time. To control the PCS/VRB unit, simultaneous active power and reactive power controlling method was developed. According to the results, it can be decided, based on by controlling the power flow exchanged between the VRB and the power system, that the proposed PCS/VRB unit works satisfactorily, the dynamic response of the control system was adequate.

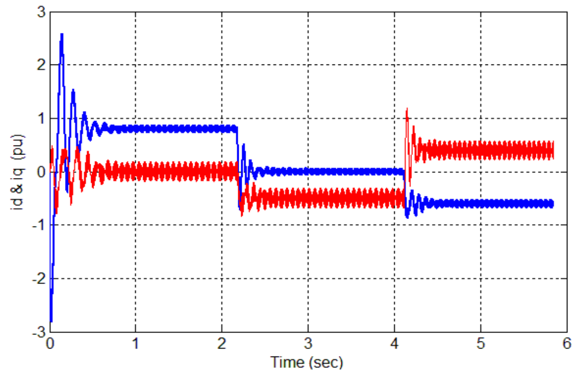

Fig. 18. i_d and i_q current in proposed model

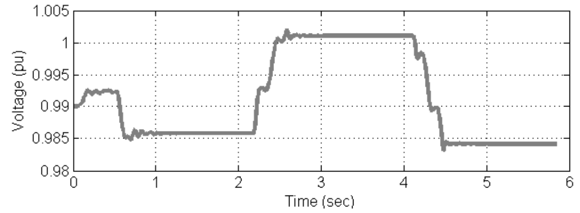

Fig. 19. voltage of the PCS/VRB unit bus

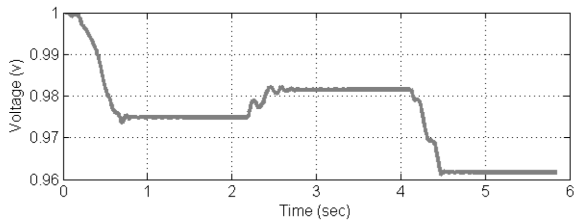

Fig. 20. voltage of 63 kV bus

References

[1] Vechiu, Ionel, et al,"Three-level Neutral Point Clamped Inverter Interface for Flow Battery/Supercapacitor Energy Storage System used for Microgrids," Innovative Smart Grid Technologies (ISGT Europe), 2nd IEEE PES Int. Conference and Exhibition on, 2011.

[2] Bingying, Wu, et al,"Optimal capacity of flow battery and economic dispatch used in peak load shifting," Electric Utility Deregulation and Restructuring and Power Technologies (DRPT), 4th Int. Conference on. IEEE, 2011.

[3] Barote, L., et al,"Stand-alone wind system with vanadium redox battery energy storage," Optimization of Electrical and Electronic Equipment, 11th Int. Conference on. IEEE, 2008.

[4] Kear, Gareth, Akeel A. Shah, and Frank C. Walsh,"development of the all vanadium redox flow battery for energy storage: a review of technological, financial and policy aspects," *Int. Journal of Energy Research*; vol. 36.11, pp. 1105-1120, 2012.

[5] Gattrell, M., et al,"Study of the mechanism of the vanadium 4+/5+ redox reaction in acidic solutions," *Journal of the Electrochemical Society*; vol. 151.1, pp. A123-A130, 2014.

[6] Banham-Hall, Dominic D., et al,"Flow batteries for enhancing wind power integration," Power *Systems, IEEE Trans.* on vol. 27.3, pp. 1690-1697, 2012.

[7] Ontiveros, Leonardo Javier, and Pedro Enrique Mercado,"Thyristor-based flexible ac transmission system for controlling the vanadium redox flow battery," *IET Renewable Power Generation*; vol. 7.3, pp. 201-209, 2013.

[8] Xiao, Xi, et al,"A Two-level Energy Storage System for Wind Energy Systems," *Procedia Environmental Sciences*; vol. 12, pp. 130-136, 2012.

[9] Barote, L., and C. Marinescu,"A new control method for VRB SOC estimation in stand-alone wind energy systems," Clean Electrical Power, Int. Conference on. IEEE, 2009.

[10] Anderson, Travis M., et al,"MetILs: a family of metal ionic liquids for redox flow batteries," 2012.

[11] L. Wei, and G. Joos, "A power electronic interface for a battery supercapacitor hybrid energy storage system for wind applications," Power Electronics Specialists Conference, PESC, IEEE, 2008.

[12] M. Shinichi, and N. Tokuda, "Vanadium redox-flow battery for a variety of applications," IEEE Power Engineering Society Summer Meeting, vol. 1, 2001.

[13] Baccino, F., et al, "Power and energy control strategies for a Vanadium Redox Flow Battery and wind farm combined system," Innovative Smart Grid Technologies (ISGT Europe), 2nd IEEE PES Int. Conference and Exhibition on, 2011.

[14] Barote, L., C. Marinescu, and M. Georgescu, "VRB modeling for storage in stand-alone wind energy systems," *Power Tech*, IEEE Bucharest, 2009.

[15] Chahwan, J., C. Abbey, and G. Joos, "VRB modelling for the study of output terminal voltages, internal losses and performance," Electrical Power Conference, EPC IEEE Canada, 2007.

[16] Li, M-H., T. Funaki, and T. Hikihara, "A study of output terminal voltage modeling for redox flow battery based on charge and discharge experiments," Power Conversion Conference-Nagoya, PCC'07. IEEE, 2007.

[17] Shibata, Akira, Sato Kanji, and Masato Nakajima, "Development of vanadium redox flow battery for photovoltaic generation system," Photovoltaic Energy Conversion, Conference Record of the 24th IEEE Photovoltaic Specialists Conference, IEEE First World Conference on. Vol. 1, 1994.

[18] Tokuda, Nobuyuki, et al, "Development of a redox flow battery system," *Sumitomo electric technical review*-english edition, 1998, pp. 88-94.

[19] Wei, Qi , Liang, Xintao, Liu, Changyuan, Nie, Tingzhi, "Research on the combined control method for parallel inverters control of micro-grid," 7th International Forum Strategic Technology (IFOST), 2012, pp. 1-5.

[20] Dragicevic, T., Guerrero, J.M., Vasquez, J.C., Skrlec, D, "Supervisory Control of an Adaptive-Droop Regulated DC Microgrid with Battery Management Capability," *IEEE Trans. on Power Electronics*, vol. 99. pp. 1-12, 2013.

[21] Gabash, Aouss, and Pu Li, "Active-reactive optimal power flow in distribution networks with embedded generation and battery storage," *Industrial Electronics, IEEE Trans. on Power Systems*; vol. 27.4, pp. 1-10, 2012.

[22] Guerrero, Josep M., et al, "Control strategy for flexible microgrid based on parallel line-interactive UPS systems," *Industrial Electronics,* IEEE Transactions on vol. 56.3, pp. 726-736, 2009.

[23] Peng, F. Z., George W. Ott Jr, and Donald J. Adams, "Harmonic and reactive power compensation based on

the generalized instantaneous reactive power theory for three-phase four-wire systems," *Power Electronics*, IEEE Trans. on vol. 13.6, pp. 1174-1181, 1998.

[24] Mohod, Sh. W. and M. V. Aware, "Micro wind power generator with battery energy storage for critical load," *Systems Journal*, IEEE vol. 6.1, pp. 118-125, 2012.

[25] Guerrero, Josep M., et al, "A wireless controller to enhance dynamic performance of parallel inverters in distributed generation systems," *Power Electronics*, IEEE Trans. on vol. 19.5, pp. 1205-1213, 2004.

[26] Guerrero, Josep M., et al, "Output impedance design of parallel-connected UPS inverters with wireless load-sharing control," *Industrial Electronics*, IEEE Trans. on vol. 52.4, pp. 1126-1135, 2005.

[27] Chen, Zhong, Ming Ding, and Jianhui Su, "Modeling and control for large capacity battery energy storage system," Electric Utility Deregulation and Restructuring and Power Technologies (DRPT), 4th Int. Conference on. IEEE, 2011.